Flow Behavior of the Liquid/Powder Mixture, Theory and Experiment: I. Effect of the Capillary Force (Bridging Rupture)

By: Yakov Rabinovich[1], Madhavan Esayanur[1, 2], Kerry Johanson[1], Chen-Luh Lin[3], Jan Miller[3], Brij M. Moudgil[1, 2,]

Abstract

Employing the equality of the mechanical work of shear stress and the energy of liquid bridges, a formula is developed for shear stress τ and unconfined yield strength f_c of compressed powder, consisting of mono-sized solid particles mixed with oil. This formula predicts the dependence of shear stress and unconfined yield strength on the oil weight fraction, C, and the radius of the particles, R, as τ and $f_c \propto$ sqrt $(C)/R$. Experimental data obtained with a Schulze cell were used to validate the developed formula. Experimental dependence of f_c on R confirms the theoretical formula. However, the experimental dependence of f_c on oil weight fraction C does not agree with the theory developed, especially at low C. Therefore, the theoretical model needs modification. Despite some approximations, the theory predicts certain features, which can be important for transport of the stressed powder/ oil mixture.

KEYWORDS: Powders, Transport process, Colloid phenomena, Unconfined yield strength, Capillary force, Desegregation

[1] Particle Engineering Research Center, University of Florida, Gainesville, Florida, USA.
[2] Department of Materials Science and Engineering, University of Florida, Gainesville, Florida, USA
[3] Department of Metallurgical Engineering, University of Utah, Salt Lake City, Utah, USA

1. Introduction

The mechanical properties of bulk powders are an important subject for experimental and theoretical research of Reed [1]. Industry has a reasonable ability to predict process behavior assuming bulk flow properties are measured at the appropriate process conditions and bulk-handling designs are based on sound theoretical approaches. Thus, the relationship between material flow properties and process behavior is often a matter of reasonable well-established engineering design principles. However, the problem with this approach is that changes in upstream particle production processes cause bulk materials to change particle size distribution, moisture content, and surface activity. These particle scale properties have significant influence on the bulk scale material flow properties. Thus, any change in process conditions can result in a material that may not flow through the existing process, resulting in hang-up conditions and decreasing productivity. One solution is to measure bulk flow properties under all possible combinations of process conditions and design for the worst situation. Unfortunately, this is often impractical or even impossible since the process must exist and be reliably producing product, which can be tested to measure the flow properties in the first place. Another approach would be to measure the flow properties of given bulk material consisting of a known moisture content, particle size distribution, and surface activity and then use a model to predict or extrapolate the effect that changes in these particle scale properties would have on the basic flow properties. This approach would allow process models to be developed that include changes in particle scale properties and allow feed forward process controls to be used in powder processes.

In addition, using models relating particle scale properties to bulk flow properties will allow product design during initial formulation stages. Ultimately engineers would then be able to optimize any product for use in a prescribed process or handling system without resorting to extensive pilot scale validation of the process. Processes currently handling powder often require significantly longer start-up schedules to achieve reliable throughput than processes not handling powders. Therefore, the development of models capable of predicting bulk flow properties, for given particle scale properties, is of paramount importance in both process and product design. This new approach to predict process behavior will help prevent cohesive flow stoppages and assist engineers in designing powders with sufficient cohesion to prevent or minimize segregation during processing and handling. For example, adding a liquid binder to bulk material has been successful in reducing segregation in food, chemical, and pharmaceutical industries. The binder produces liquid bridges between particles, which help to avoid powder segregation.

The bulk flow property causing the most difficulty in predicting process behavior is unconfined yield strength, f_c. This bulk property is defined as the major principal stress acting on an unconfined bulk material that produces failure of the bulk material through shear. A typical result from consolidation and fail of a powder sample is shown in Figure. 1. The corresponding points on the Mohr circle and shear stress time series are shown to illustrate the procedure of generating the yield locus. Yield locus concept shows relationship between strength, f_c, major principal stress σ_1, and internal friction angle ϕ. Yield strength of powders depends on the consolidation stress, σ_1, applied to the material. Generally, the larger the consolidation stress, the larger the unconfined yield strength. Associated with an unconfined yield strength value, f_c, at a particular consolidation stress, σ_1, is a yield locus. This locus represents the collection of all the shear and normal stress points that will cause incipient failure of the bulk material, which has been pre-consolidated to a major principal stress of σ_1. In fact, measuring this yield locus using

direct shear testers provides the means of determining unconfined yield strength. The details of this methodology will be discussed below.
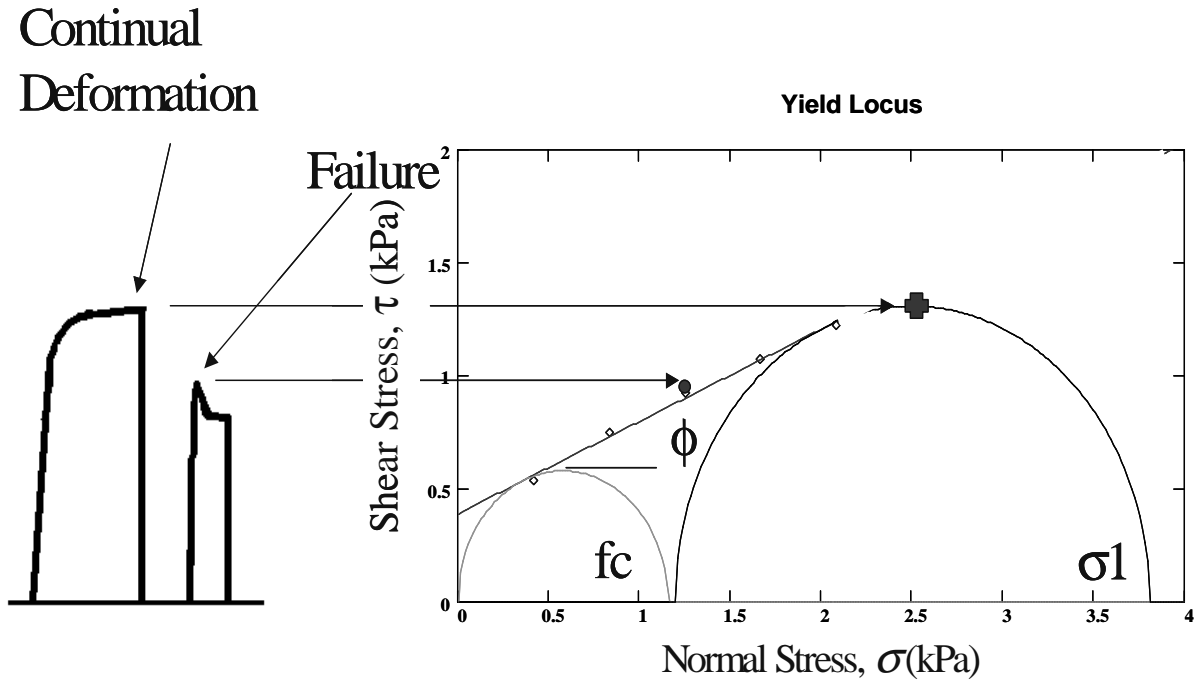

Figure 1. Yield locus and shear stress time series concept showing relationship between strength, f_c, major principal stress σ_1, effective internal friction angle, δ, and internal friction angle ϕ

Another way of describing the strength of a bulk material would be to recognize that the unconfined yield strength can be thought of as a resistance to shear of a collection of particles, each subjected to a set of contact adhesive forces and surface friction forces during inter-particle motion. The vector sum of these forces divided by the appropriate area would yield an estimation of the shear stress acting during failure and steady shear. For wetted particles, initial liquid bridges would form between adjacent particles and the liquid would be drawn to zones where the inter-particle gap is smallest due to capillary force. The initial shear deformation of the particle assembly will break the largest number of liquid bridges. Thus, the initial shear force would be the greatest corresponding to the peak stress observed during initial failure. These liquid bridges would then break and reform in a non-simultaneous manner during subsequent shear generating steady state shear stresses. If all of the forces acting between the particles were known and the initial position of particles were known then Newton's laws of motion could be applied to the collection of particles and the movement of the particle system be predicted. This is the basis of the discrete element method (DEM).

3

DEM provides a reasonable approximation to the shear and normal stresses acting on the bulk assembly of particles. It will produce an approximation to the motion of particles in the system when these particles are perturbed by the motion of a wall or other boundary. Thus, the effect of wall properties on bulk behavior can be evaluated. The method also allows calculation of a powder coordination number under normal stress conditions. Unfortunately, DEM is very calculation intensive and only as accurate as the inter-particle force laws that are used in the simulation calculations. Moreover, DEM demands knowledge of the elastic properties of particles and some hypothesis about adhesion (cohesion) force between particles.

Another approach has been suggested by Johanson et. al. [2] and is based on the calculation of inter-particle separation energy rather than maximum contact forces. This previous work suggested a qualitative formula allowing evaluation of unconfined yield strength (f_c) for powder with oil under normal (σ) and shear (τ) stresses. In these calculations it was suggested that mechanical work of shear stress is equal to the rupture energy of liquid bridges (annuluses) between particles. As a result of this hypothesis, the following qualitative formula was developed.

$$f_c \propto \frac{\sqrt{C}}{R}$$ where C is liquid weight fraction and R is particles radius.

Due to the qualitative character of this formula, quantitative conclusions about the powder behavior were not possible. In the present paper, taking into account the rupture energy of the liquid bridges, a formula is developed which allows quantitative calculation of f_c and τ, i. e., the ability to predict the unconfined yield strength of a mixture of the solid powder and liquid.

2. Direct shear test methodology

This new analysis starts with a discussion of direct shear testing using the Schulze cell [3], which was used to measure the yield locus of materials containing liquid binders. This standard shear cell is an annular direct shear cell, which is represented schematically in Figure. 2. The description of the shear cell, method of obtaining Mohr circles and measurement of unconfined yield strength, f_c, are given in Addendum. The major principal stress (σ_1) is determined by drawing a Mohr circle through the critical stress state and tangent to the yield locus.
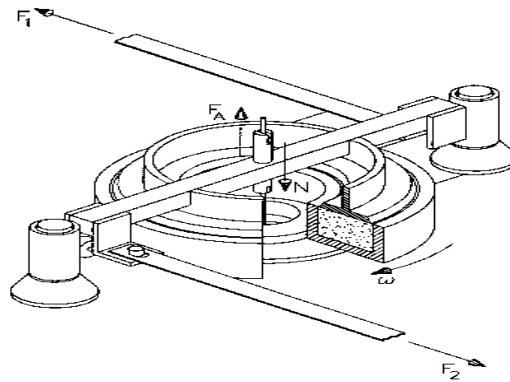

Figure 2.   Schematic of the Schulze cell. The annular region of the cell is filled with powder with the two load arms connected to the stationary top. The bottom of the cell is rotated to shear the sample consolidated by applying different normal loads

This entire process of obtaining Mohr circles is repeated several times for each per-consolidation stress allowing the latter to vary. Thereby several yield loci are generated. There exists a strength and consolidation point for every unique yield locus. These unique strength points are plotted as a function of major principal stress associated with the critical state of stress. This plot is known as the flow function and is used to predict process behavior of cohesive materials. Such a plot exists for glass beads mixed with oil in previous work done by Johanson et al. [2]. This data is used in this paper to extend and validate the theory for predicting unconfined yield strength from liquid binder content and particle size data.

3. Experiment: Materials and Methods

The mono-dispersed glass particles ("spheriglass") with different sizes (diameters) between 72 and 1000 µm were supplied by Potters Industries Inc. In agreement with a supplier data, the size distribution can be characterized by the values of D_{50}, D_{90} and D_{10}. For example, for particles with median diameter D_{50}=116 µm, these values are, as D_{10}=93 µm and D_{90}=141 µm."

White mineral oil of "Sharpening Stone" grade was obtained from Norton Co., Littleton, NH, USA. The viscosity of oil was 25 cP, as measured by capillary viscometer, surface tension was γ=27 mN/m. The contact angle of oil on glass surfaces ranged from 0 to 10°.

Oil was added to the bulk material by measuring the weight of oil in an atomizer. The oil was then sprayed on the bulk material as it was mixed in a small rotary shaft mixer for five minutes. The quantity of oil in the mixture was determined by weighing the atomizer bottle before and after oil addition. Visual microscopic observations were made to ensure that the oil was well distributed in the bulk mixture.

The dimensions of Schulze cell are, as following, the outside- and inside diameters are 20 cm and 10 cm, respectively, the height is near 2 cm. The strength measurements were done in the standard cell with powder material. Thus they are accurate and done in accordance with the ATSM standard. The velocity measurements were measured using x-ray tomography in a smaller cell to provide better resolution at the particle scale. The size of the cell is 40 mm outside diameter and 32 mm inside diameter. The annular space in the cell was 10 mm with a depth of 10 mm. X-ray tomography can provide a 2% to 5% spatial resolution. With respect to the resolution, the reconstruction was done with a voxel resolution of 80 microns. Thus the smaller cell has a benefit. Please note that the number of particle diameters in this small scale shear cell was in accordance with the number or relative size of particles addresses in the ASTM standard to achieve reasonable shear results.

4. Results and discussion

4.1. Particle scale theory for predicting strength

Consider the behavior of the powder in the Schulze cell [3] under normal and shear stress. This behavior mimics the transport properties of powder through bins and hoppers. To relate the mechanical properties of the powder mixed with liquid with properties of the liquid bridge between individual particles, one of two alternative hypotheses can be chosen. The first hypothesis is that in the process of powder shearing, maximal attractive (adhesion) forces act during liquid bridge breakage. The second hypothesis is that the work, caused by lateral (shear) stress, is equal to the energy needed to break the liquid annuli between particles. The first

hypothesis leads to conclusions that unconfined yield strength should be independent of oil weight fraction (weight fraction), *C,* because maximal capillary adhesion force (at the distance between particles *H*=0) in agreement with Haines [4] and Fisher [5] is independent of the annulus volume, *V,* and therefore of *C.* The first hypothesis contradicts previous experimental data obtained for powder from quartz or glass particles [2, 6]. The second hypothesis about correlation between work of adhesion and work of shear stress leads to the following.

Energy of the annulus can be calculated as the integral of the force/distance dependence relationships, which in turn can be determined from the paper of Rabinovich et. al. [7]. On the other hand, the energy of one annulus with small fixed volume is given directly by Israelachvili [8], as the following Eq. 1,

$$E_1 = 2\pi\gamma R^2 \cos\theta \cdot \alpha^2 \qquad (1)$$

where γ is the liquid surface tension, θ is the contact angle and α is the half-embracing angle (Figure. 3). Israelachvili [8] obtained this formula calculating the difference between free energy of dry solid surface and energy of surface coated by liquid. The validity of Eq. 1, despite the non- equilibrium character of the capillary force with the constant volume bridge, was confirmed by Rabinovich et. al. [6, 7] theoretically and experimentally.
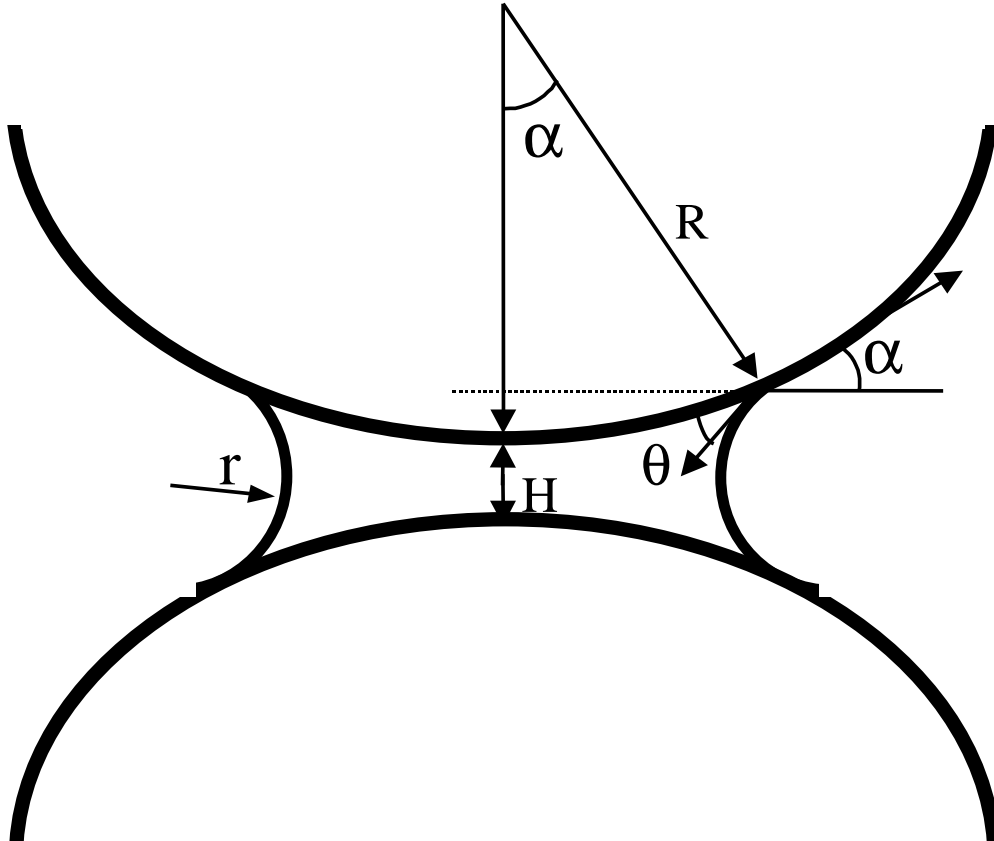

Figure 3.   Geometry of the liquid bridge between two spherical particles

The present discussion allows the correlation between the energy of annulus breakage and the powder yield strength. The calculation of the annulus energy with Eq. 1 requires knowledge of the value of the bridge embracing angle, α, or the bridge volume, V_l, which is related to α. For powder mixed with oil, this volume, V_l, can be found if the weight fraction of oil in powder (C) is known, as follows:

$$V_1 = \frac{8\pi R^3 C \rho_{sol}}{3n \rho_{oil}} \tag{2}$$

where C is weight fraction of oil, the density of oil, ρ_{oil}, is equal to 0.95 g/cm^3 and ρ_{sol} is the solid density (ρ_{glass}= 2.5 g/cm^3) and n is the number of the oil annuluses associated with each glass particle (coordination number). Eq. 2 takes into account that each annulus belongs to the pair of particles. In Eq. 2 (and in Eqs. 5 and 9 below) we imply that whole volume of liquid is found in the liquid bridge. It is almost correct for oil on silica surface, because in this case the pressure inside oil is almost equal to atmospheric one (minus dispersion force silica/oil/air) while in bridge (under curve meniscus) the pressure is lower than atmospheric one. However, due to kinetic reasons (viscosity), part of oil remains in film. This yields to overestimated values of V_l in Eq. 2 and f_c in Eq. 9. Another problem is that not every contact point is filled by oil bridges. Moreover, different bridges have different volumes. In the present paper we don't consider these effects because their including would make theory too complex and demand involving additional unknown fitting coefficients.

For contacting particles (the shortest distance H=0) the bridge volume is related to the embracing angle, α, as suggested by Rabinovich et al. [6, 7]:

$$\alpha^2 = \sqrt{\frac{2V_1}{\pi R^3}} \tag{3}$$

The total number of bridges (N) per unit volume (V) is [9]

$$\frac{N}{V} = \frac{3k_r n}{8\pi R^3} \tag{4}$$

where random volume packing factor is k_r=0.64 (i.e., the portion of the total volume filled by particles), as suggested by Jaeger and Nagel [10]. Similar to Eq. 1, Eq. 4 also takes into account that each bridge belongs to two particles.

Suppose that only a certain portion p of available liquid bridges is broken, while the rest of the particles bridges remains intact during shear. The energy E needed to rupture liquid bridges per unit volume during shifting for one elementary (unit) step, is obtained from Eqs.1 to 4, and given in Eq. 5.

$$\frac{E}{V} = 3\gamma\cos\theta \cdot k_r \cdot p \cdot \sqrt{\frac{C\eta\rho_{sol}}{3\rho_{liq}}} \qquad (5)$$

where the elementary step distance, l, is given by Eq. 6.

$$l = 2R \qquad (6)$$

Note that this equation gives only the first approximation for the elementary step, because the actual distance between particles depends on the packing type. Note also that if rupture occurs at smaller distance than elementary step, then probability coefficient p in Eq. 9 decreases, but theory developed still will be valid. Fitting coefficient p in Eq. 5 takes into account not only portion of the broken bridges, but also possibility of simultaneously reforming bridges, which number should be subtracted form the number of broken bridges.

On the other hand, the mechanical work (W) during shear at a shear stress (τ) for the shift of unit volume of n_l-layers of particles for the elementary step with respect to each other can be calculated as follows:

$$W/V \equiv W/(An_l l) = \tau/n_l \qquad (7)$$

Where A is an area of the horizontal layer (failure plane) of Shulze cell (see Figure. 2). Here incremental approach is suggested when shear stress between two layers equal τ/n_l. The Mohr circle geometry implies the following relationship between yield strength f_c and shear stress τ along the failure plane:

$$f_c = \frac{2 \cdot \tau}{\cos\phi} \qquad (8)$$

where ϕ is the internal angle of friction given by the slope of the yield strength locus in the Mohr circle diagram (Figure 1). Making the assumption that mechanical work, W, should equal liquid bridge rupture energy, E, and using Eqs. 5, 7 and 8, the following final formula for the unconfined yield strength is obtained:

$$f_c = \frac{6\gamma\cos\theta \cdot k_r \cdot n_l \cdot p}{R\cos\phi} \sqrt{\frac{C\eta\rho_{sol}}{3\rho_{liq}}} \qquad (9)$$

It is important to note the following approximations made for the development of this formula and restrictions for its application: the formula is valid only for a small volume of the liquid bridges as compared with the particle volume; no friction is taken into account; the powder is suggested to be mono-dispersed; the volume of each liquid bridge is considered to be the same; all particle contacts considered contain liquid bridges (i.e., there are no dry contacts); all liquid exists in the bridges and there is no liquid film on the particle surface; and the shear stress

changes linearly through n_l- layers of the powder. The approximation for small bridge volume is valid almost always. However, the friction force can not actually be neglected, especially under low or zero humidity.

Note that only at very low concentrations of liquid, C, the volume of bridge V_1, calculated with Eq. 2, is too small to create bridge [11]. As it was shown in Ref. [11], in the case of water the minimal radius of meniscus, when the bridge volume could be considered as phase (rather than monolayer) and when the conception of surface tension is valid, r min=0.5 nm. The corresponding minimal volume of liquid bridge can be calculated for various radius of particle. For lower concentrations, only part of contact points will be filled by liquid and Eq. 9 is not valid. Note also, that for very low concentration of liquid, Eq. 9 is not valid also for another reason. Namely, we did not involve in theory the friction force, which plays major role at low liquid concentration. This problem is considered in the second part of the present paper.

Monodispersed particles can be used in laboratory (as it was in the present paper) rather than in industrial processes. Advanced model taking out other restrictions should be developed in the future papers.

Equation 9 predicts the correlations between the unconfined yield strength, f_c (or unconfined shear stress, τ), and weight fraction of oil, C, and radius of particles, R. Moreover, this equation expresses the yield strength as a function of the proportion (p) of broken bridges in the shear layer. Validation of this equation was performed by measuring number of shear layers, n_l, and measuring the yield strength, f_c, using experimental data obtained with Schulze cell.

4.2. Number of shear layers

The number of particle layers, n_l, involved in shear is an important parameter in the predictive strength equation. This parameter is used to estimate the number of particles involved in rupture of liquid bridges during shear. To compare experimental results for unconfined yield strength with theory (Eq. 9) we should know independently at least one of two parameters, the number of shear layers, n_l, or the probability of bridge rupture, p. X-ray micro-tomography developed by Lin and Miller [12] at the University of Utah provided the important information on the formation of the shear zones within a shearing powder sample in a specially designed micro-ring shear tester, similar in construction to the Schulze cell. This small-scale cell was used to observe the thickness of the shear layer during failure and estimate the number of moving particle layers (n_l) in a glass powder. The powder used in this experiment was ground glass with 5% fine iron oxide particles that were introduced as a tracer into the cell. The material in the cell was compacted and the base was manually turned using a rotary stage to shear the bulk material in the cell. The position of markers was tracked at stages during the shear process and the relative displacements of iron markers were computed as a function of depth in the test cell.

The relative motion of particles and the width of the shear zone were analyzed using results of Lin and Miller [12] of x-ray micro-tomography capable of obtaining three-dimensional images of powder samples. The relative angular movement of the dry ground glass particles with radius near 25 μm is shown in Figure. 4 as a function of height of the shear cell. It is important to note that this figure shows three distinct slopes in the angular displacement of material as a function of material height in the cell. The region between a height of 6 mm to a height of just over 7 mm shows almost a 3 degrees change in angular displacement. The displacements below and above this zone are likely due to local consolidation of the material during shear but do not represent a significant relative motion of particles during shear. This distinct displacement zone between 6

and 7 mm was taken to be the active shear zone in the tester. Histograms of the angular displacement of observed particles in different zones suggest an average angular displacement of 2 degrees in the lower section of the test cell while the top material is displaced approximately 5 degrees. The shear-zone was identified and marked as the "effective shear zone", which was determined to be equal 1.5 mm of height, corresponding in the first approximation to 30 particle layers. (Note, that here we suggested the distance between layer to be equal to $2R$. Actual distance depends on the type of packing. Change of the precise number of layer yields to the change of the probability of p in Eq. 9, which is fitting parameter in the present paper, but does not influence of the suggested theory.) A similar result was obtained using a slice model to approximate shear zones in the Jenike cell. Therefore, the number of particle layers, n_l, used to predict unconfined yield strength, f_c, from Eq. 9 was set equal to 30. Typical literature shear layers values, n_l, for glass [13-18] were found to be in the range $n_l = 4$ to 18; Janssen et. al. [19, 20] found n_l equal 1000. The present experimental value seems to be reasonable.
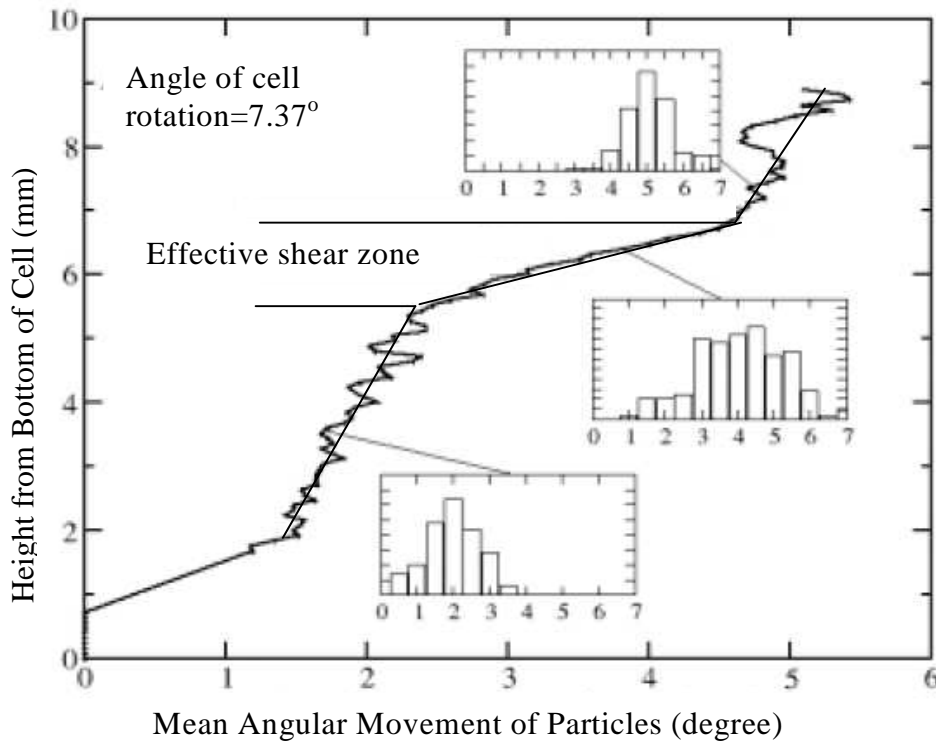

Figure 4. *Mean angular displacement of glass particles along the height of micro- ring shear tester. Radius of particles is 25 μm. The sudden change in slope of this figure identified as the "effective shear zone" represents the size of the failure zone in the test cell. Results show the size of the shear zone to be near 1.5 mm, which corresponds to about n_l=30. Histograms in the figure relate to the probability of the angular movement of particles at the certain height in the tester*

4.3. Estimation of coordination number

The coordination number also affects the prediction of unconfined yield strength. Estimations of the coordination number were determined using a DEM approach. The Discrete Element Method (DEM) is used to simulate the current system of spherical particles in the Schulze shear cell. The exact geometry of the shear cell was used and the particles were allowed to rain down into the cell. After deposition of the particles, the system was packed by simulated shaking of the cell. The contact (coordination) number for each particle in the loose packed state was determined. The distribution (histogram) of the coordination number, obtained for the packing density of 0.4, is plotted in Figure. 5. As a result, the coordination number (n) used in the prediction of unconfined yield strength from Eq. 9 was equal to 8.0.
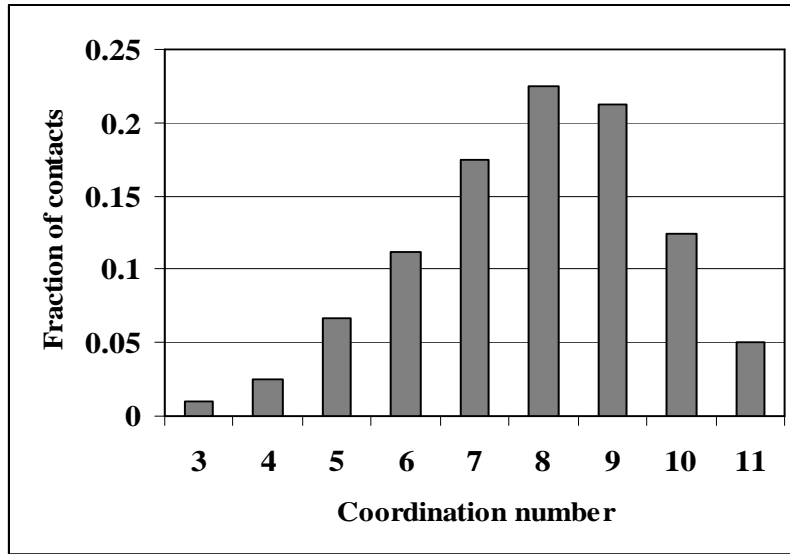

Figure 5.   DEM- diagram of coordination number in monosized powder with volume packing fraction 0.4

4.4. Results of Schulze tests

The Schulze cell was used as described above to measure the unconfined yield strength as a function of the major consolidation stress for various glass bead particle sizes and oil contents. This information was required to generate typical flow functions for glass bead mixtures. Although flow functions are very useful in predicting process behavior, it is difficult to see the relationships between strength and binder weight fraction and strength and particle size. In order to determine these relationships, strength values at prescribed major stress conditions were interpolated and the strength data were plotted as yield strength as a function of binder weight fraction (for a given particles radius) and as a function of particle size (for a given binder weight fraction). Figures 6 and 7 contain the results of these tests for glass beads with oil added as the binder.

Results for the experimental dependence of the yield strength f_c (points) on the particle size (diameter) at oil weight fraction $C = 0.001$ (=0.1%) and major principle stress $\sigma = 2$ kPa are given in Figure. 6. The solid line corresponds to the results from Eq. 9 with the parameter values given

in the figure caption. Note, that to fit the experimental data by the theoretical line the best fit value of probability of the bridge rupture (i.e., the probability of the mutual movement of particles) was obtained equal to $p=0.127$. This probability number is less than one and implies that each particle breaks a unique liquid bridge for every five that are involved in the shear zone. This could occur if the bulk material shears in agglomerates containing several adjacent particles rather than shearing occurring between individual particles. Note also, that the linear character of the experimental dependence of f_c vs. $1/R$ demonstrates that the flow parameters in Eq. 9 (n, n_l, p) are independent of R.
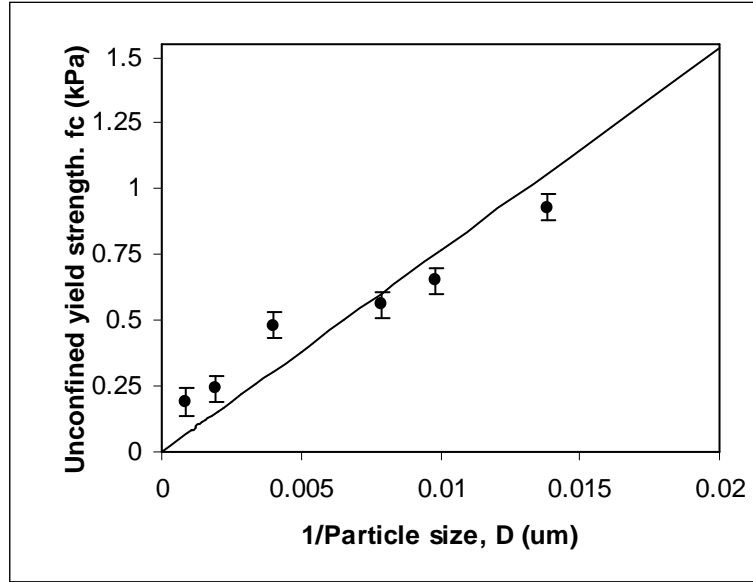

Figure 6. *Unconfined yield strength as a function of the reciprocal diameter (1/D) for oil content of 0.1% and a major normal stress $\sigma= 2 kPa$. The points are experimental data and the solid line is plotted with the theoretical Eq. 9 with the following parameters: $\rho_{sol}=2.5 \cdot 10^3 kg/m^3$, $\rho_{liq}=0.95 \cdot 10^3 kg/m^3$, $\gamma=27 mN/m$; $n=8$; $k_r=0.64$; $n_l=30$; $\varphi=30^o$, $\theta=0^o$, the fitting value of $p=0.127$. The linearity of graph proves the independence of the parameters value of the particles radius*

The dependence of (f_c) on the other parameter, the oil weight fraction (C) is shown in Figure. 7. Fitting the experimental data by Eq. 9 (with the best fitting parameter $p=0.168$) gives a poor result because the theoretical line predict to go through the coordinate origin, which contradicts the experimental data. Moreover, the value of the best fit parameter $p=0.168$ does not coincides with the fitting value of $p=0.127$, obtained above form the dependence of f_c vs. R (Figure.6). It means that the present theory (Eq. 9) needs modification. The theory can be improved by introducing additional inter-particle forces besides those caused during the rupture of the oil bridges. Particularly, the inclusion of the friction force should significantly increase the yield strength for dry powder (i.e., at $C=0$). This model is developed in the second part of the present paper.
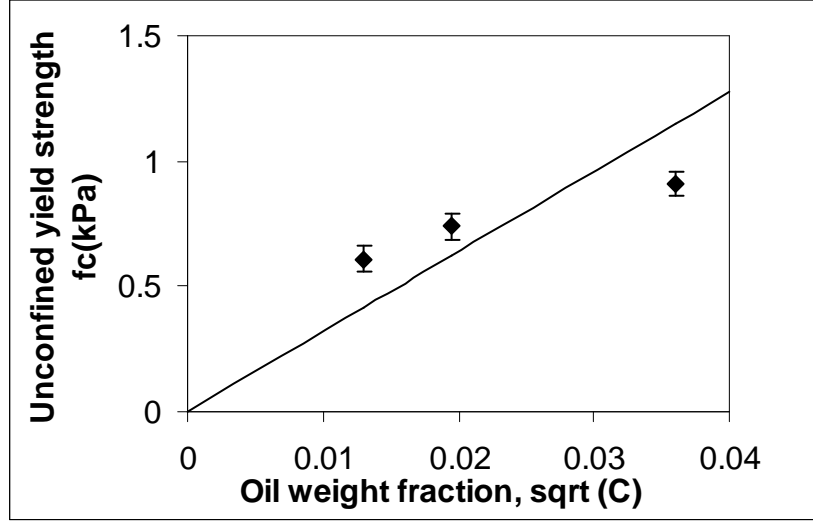
Figure. 7. Unconfined yield strength of 100 μm diameter glass beads vs. the weight fraction of oil. The points are experimental data and the solid line is Eq. 9 with the best fitting parameter p=0.168. The latter does not coincide with the fitting value of p=0.127, obtained from Eq. 9 and the experimental dependence of f_c vs. 1/D (Figure. 6). Eq. 9 gives poor fit for experimental dependence f_c vs. C. The disagreement of the experimental data and the theoretical Eq. 9 means that improved theoretical model should be developed

Despite the restrictions mentioned above, the developed theory predicts, at least semi-quantitatively, the correct character of the dependence of f_c on R and, therefore, suggests the qualitative correctness of the "energetic" approach used in the present paper for investigation of the flow behavior of the solid/liquid mixture under normal and shear stress. Moreover, the linearity of the dependences of f_c vs. 1/R and sqrt(C) proves that the values of the parameters (n, n_l, and p) don't depend on the radius of particles and the oil weight fraction. It allows prediction the yield strength of the liquid/ powder mixture.

5. Conclusions

Equating the shear stress mechanical work and the energy of liquid bridge rupture, a formula has been developed for the unconfined yield strength of a liquid/ particle mixture as evaluated in a Schulze cell. The theory predicts that unconfined yield strength (fc) is, as follows,

$$f_c = \frac{4 \cdot \gamma \cdot \cos\theta \cdot k_r \cdot n_l \cdot p}{R \cdot \sqrt[3]{k_h} \cdot \cos\phi} \sqrt{\frac{C \cdot n \cdot \rho_{sol}}{3 \cdot \rho_{liq}}} \propto \frac{\sqrt{C}}{R} \qquad (10)$$

where (C) is weight fraction of the liquid and (R) is the particle radius. The application of the formula is restricted by small liquid volume, which is correct for the modern humidity. All bridge volumes are suggested to be the same and particles are mono-dispersed.

Experimental measurements of the yield strength in Schulze cell confirmed the linear correlation of f_c and 1/R, but disproved the theoretically predicted linear correlation with sqrt (C). Despite

limitations, the theory predicts certain features for the failure behavior of powder. As a result, the obtained formula can be applied to predict flow properties of powder particles mixed with oil to avoid segregation or give estimates of the tendencies for moist material to form hang-ups in process equipment.

6. List of symbols

A- area of shear layer, m^2
C- liquid weight fraction, g liquid/ g powder
E- energy to rupture n_l- layers of powder mixture for unit step, J
E_1- energy of one annulus, J
f_c- unconfined shear strength, Pa
H- shortest distance between particles, m
k_h- hexagonal volume packing coefficient, dimensionless
k_r- random volume packing coefficient, dimensionless
l- elementary (unit) step distance, m
n- number of oil annuli associated with each particle (coordination number)- dimensionless,
n_l- number of shear layers of particles, dimensionless
p- proportion of broken bridges, i.e. probability of the mutual shift of particles, dimensionless
R- particle radius, m
V- the volume of shifting layers, m^3
V_1- the annulus volume, m^3
W- mechanical work during shear for elementary (unit) step, J

Greek letters
α- half-embracing angle of annulus, rad
γ- surface tension, N/m
θ- contact angle, rad
ρ_{oil} - density of oil, kg/m^3
ρ_{sol} - density of solid particles, kg/m^3
σ- normal stress, Pa
σ_1- particular consolidation stress, Pa
τ- shear stress, Pa
φ- internal angle of friction, rad

7. Addendum:
Schulze cell [3] and measurement of unconfined yield strength f_c.

The cell consists of an annulus base connected to a cog, which is driven by a motor. A powder material is placed into the base and the top with protruding vanes is placed on the material. The top is connected to two load cells through two tension arms. The weight of the top and tension arms is counter balanced by a lever system above the cell. The top remains stationary while the base is rotated. This allows measurement of the torque acting on the tester top. Various weights are applied to the weight hanger connected to the top of the cell. A prescribed normal force is placed on the weight hanger and the base is rotated until shear torque on the cell reaches a constant value. This procedure generated a unique state of stress within the material known as the critical state of stress. Once the critical stress state is reached, the rotation of the base is

stopped and the normal load on the top is reduced. The base rotation is then initiated a second time and the material experiences a maximum peak shear stress causing failure of the bulk material in a zone positioned just below the vanes in the tester. It is important to point out that this failure is for the powder material, which has been subjected to a prescribed critical state of stress and then failed. All of the failures measured in this way are related to a single state of stress, which represents the critical state of stress induced during the steady shear part of the test. The maximum shear torque during failure is recorded and used to compute a shear stress value on the failure yield locus. This procedure is repeated several times to generate a collection of points on a yield locus. A curve or a line is drawn through these points and the unconfined yield strength, f_c, is obtained by drawing a Mohr circle through the origin and tangent to the yield locus.

9. References

1. Reed, J.S. Principles of Ceramic Processing. 2nd edn., John Wiley, New York, 1995.

2. Johanson, K., Rabinovich, Y., Moudgil, B., Breece, K., Taylor, H., Relationship between particle scale capillary forces and bulk unconfined yield strength. *Powder Technology*, **138** (2003) 13-17.

3. Schulze, D. Flowability of Bulk Solids- Definition and Measuring Principles. *Chemie Ingenieur Technik* **67** (1) (1995) 60-68.

4. Haines, W.B., A Note on the Cohesion Developed by Capillary Forces in an Ideal Soil. *Journal of Agriculture Science*, **15** (1925) 529.

5. Fisher, R.A. On the Capillary Forces in an Ideal Soil; Correction of Formulae given by W. B. Haines. *Journal of Agriculture Science*, **16** (1926) 492.

6. Rabinovich, Y.I., Esayanur, M.S., Johanson, Adler, J.J., Moudgil, B.M., Measurement of oil-mediated particle adhesion to a silica substrate by atomic force microscopy. *Journal of Adhesion Science and Technology,* **16** (7) (2002) 887-903.

7. Rabinovich, Y.I., Esayanur, M.S., Moudgil, B.M., Capillary force between two spheres with a fixed volume liquid bridge: Theory and experiment. *Langmuir*, **21** (24) (2005) 10992-10997

8. Israelachvili, J.N., Intermolecular and Surface Forces. 2nd Edn., Academic Press, San Diego, 1992.

9. Reed, J.S. In "Principles of Ceramic Processing." 2nd edn., John Wiley, New York, 1995. Chapter 13 "Particle Packing Characteristic", p. 318.

10. Jaeger, H.M., Nagel, S.R., Physics of Granular States. *Science*, **255** (1992) 1523-1530.

11. Y. I. Rabinovich, T. G. Movchan, N. V. Churaev, P. G. Ten, "Phase separation of binary mixtures of polar liquids close to solid-surfaces." *Langmuir*, **7** (4) (1991) 817-820.

12. Lin, C.L., Miller, J.D., Cone beam X-ray micro- tomography - a new facility for three-dimensional analysis of multiphase materials. *Minerals and Metallurgical Processing*, **19** (2002) 65- 71.

13. Scarlett, B., Todd, A.C., A split ring annular shear cell for determination of shear strength of a powder. *Journal of Physics E, Scientific Instruments,* **1** (6) (1968) 655.

14. Scarpelli, G., Wood, D.M., IUTAM Conference on Deformation and Failure of Granular Materials. Delft, 1982.

15. Oda, M., Kazama, H., Konishi, J., Effects of induced anisotropy on the development of shear bands in granular materials. *Mechanics of Materials*, **28** (1998) 103- 111.

16. Oda, M., Kazama, H., Microstructure of shear bands and its relation to the mechanisms of dilatancy and failure of dense granular soils. *Geotechnique*, **48** (1998) 465- 481.

17. Bardet, J.P., Orientation of Shear Bands in Frictional Soils. *Journal of Engineering Mechanics-ASCE,* **117** (1991) 1466- 1484.

18. Bardet, J.P., Proubet, J., A Numerical Investigation of the Structure of Persistent Shear Bands in Granular Media. *Geotechnique*, **41** (1991) 599- 613.

19. Janssen, R., Structure and shear in a cohesive powder. Dissertation for partial fulfillment of doctorate of philosophy. University of Delft, Netherlands (2001).

20. R.J.M. Janssen, B. Scarlett, W.H. Kraan, N.H. van Dijk, M.Th. Rekveldt. "Visualization of the shear region in a cohesive powder by scanning with a polarized neutron beam." *Powder Technology* **159** (2) (2005) 87-94. doi:10.1016/j.powtec.2005.01.021